



Microwave Imaging Using SAR

I. Kalantari¹ and B. Zakeri^{2*}

1-MSc. Student, Department of Electrical Engineering, Amirkabir University of Technology, Tehran, Iran

2-Assistant Professor, Department of Electrical Engineering, Babol Noshirvani University of Technology, Babol, Iran

ABSTRACT

Polarimetric Synthetic Aperture Radar (Pol.-SAR) allows us to implement the recognition and classification of radar targets. This article investigates the arrangement of scatterers by SAR data and proposes a new Look-up Table of Region (LTR). This look-up table is based on the combination of (entropy H /Anisotropy A) and (Anisotropy A /scattering mechanism α), which has not been reported up now. First of all, the color coded images of each of the quantities of H , A and α are extracted and then having the matrix associated with each image and evaluating its histogram, we could obtain the image parameter values corresponding to each interval related to each color code. Then in the output the combination of parameters and the sharing of their images of each frame are extracted and compared with optical images and the extracted satellite map of scattered fields. Results for unconventional targets such as random rough surfaces has indicated that mechanism of scattering irregularities and improper alignment can be used for different purposes in different parts of the frame with fixed values that can be a new method for identifying targets. To make a look up table it is essentially required to evaluate the target parameters and classification of radar images. The method of the extraction of these parameters and applying them on imaging radar systems is exclusive. To validate our work, Pol. SAR data sets are used.

KEYWORDS

Polarimetric radars, Decomposition theorem, Covariance matrix, Estimation theory.

*

Corresponding Author, Email: zakeri@nit.ac.ir

1- INTRODUCTION

Synthetic Aperture Radar (SAR) is a coherent imaging technique capable of generating fine resolution images of stationary target on the ground [1–3]. SAR is an important tool in military intelligence, surveillance, and reconnaissance which has been successfully applied to the remote sensing of rough surface, in all-weather [4–7]. Over the ocean scene, it is influenced by varying surface winds, waves and currents, as well as the presence of surface material and oil spill.

Classification of SAR image is one of the many important applications of polarimetric data. A systematic classification procedure will place the classification process on a more quantitative level and reduce the amount of necessary photo-interpretation. Single and multi-frequency classifications were used in the past, but classifications can now be applied to fully polarimetric data, which have become available due to recent developments in radar technology.

In 1997, start to use target decomposition for POLSAR image classification, cloude raised his famous H/ α classification algorithm based on scattering entropy H and scattering angle α , derived from cloude decomposition model [8]. In 1998, Lee et al, proposed Wishart H/ α unsupervised algorithm, which combines H/ α model and the statistical property of scatter matrix [9]. Its better result comes from cyclic iterative method in Wishart clustering model with H/ α classification result as initial value. During 2000 and 2002, Pottier et al, put forward Wishart H/ α /A algorithm, by adding anisotropy A as further improvement of Wishart H/ α model [10-13].

Scattering properties offered a better model comprised of freeman decomposition and Wishart classifier [14-16]. In [16], the estimation of the polarimetric signatures including the combination of target decomposition and the maximum-likelihood estimator is presented. In some cases, the absolute magnitude and phase of the radar return and are not reliable features for data classification purposes. Therefore, many previous methods on the classification of radar images of targets may not represent accurately.

In this paper, a great agreement of the work has been focused on detection and classification of targets based on the parameter values of H, A and α . Two separate tables is proposed to detect targets with precision targets such as sea areas, vegetation areas, buildings and coast regions. A new hybrid method has been obtained by using pairs of these parameters leading to updating the previous known look-up table. Consequently, two new look-up tables are achieved by H/A and A/ α .

In section 2, we introduce theoretical analysis of the target decomposition (TD) and the concept of Pauli Distribution (PD). In section 3, the experiments by using the NASA/JPL AIRSAR images are presented. Identification experiments and the associated results will be provided in Section 4. Before last section the look-up tables, classification results and comparisons with a new area are shows. The last section provides the conclusion of this paper.

2-THEORY

2-1-BASIC THEORY

To assess distributed targets such as natural scatterers, we consider an arbitrary randomly rough surface (RRS). According to this, in vector representation, the linear combination of two perpendicular polarizations of a single frequency plane wave issued. When a horizontal or vertical polarized wave hits a target, the backscattered wave can have contributions in both horizontal and vertical polarizations. The backscattering matrix of a target can be completely described as [18]:

$$s = \begin{bmatrix} S_{hh} & S_{hv} \\ S_{vh} & S_{vv} \end{bmatrix} \quad (1)$$

In order to find the second order descriptor of targets or namely the coherency or covariance matrices, initially, we must calculate the scattering vector k_p , which can be represented for reciprocal media as:

$$k_p = \frac{1}{\sqrt{2}} [S_{hh} + S_{vv} \quad S_{hh} - S_{vv} \quad 2S_{hv}] \quad (2)$$

The coherency matrix is related to the target vector as:

$$[T] = k_p \cdot k_p^{*T} \quad (3)$$

Using coherency matrix analysis, Cloude and Pottier proposed an eigenvector decomposition model, using scattering mechanism α , entropy Hand anisotropy A [13].

2-2-PAULI TARGET DECOMPOSITION

When a horizontal or vertical polarized wave is incident upon a target, the backscattered wave can have contributions in both horizontal and vertical polarizations. The features are derived from the multi-look coherence matrix of the polarimetric SAR data. Suppose S stands for the measured scattering matrix. Here, S_{ij} represents the scattering coefficients of targets, i the polarization of the incident field, j the polarization of the scattered field. In mono-static radar systems, because the reciprocity applies in a mono-static radar system configuration $S_{vh} = S_{hv}$ and then the scattering matrix is defined by [10]:

$$s = \begin{bmatrix} S_{hh} & S_{hv} \\ S_{hv} & S_{vv} \end{bmatrix} = \alpha [s]_a + \beta [s]_b + \gamma [s]_c \quad (4)$$

where

$$\alpha = \frac{S_{hh} + S_{vv}}{\sqrt{2}} = \frac{S_{hh} - S_{vv}}{\sqrt{2}}, \gamma = \sqrt{2} S_{hv} \quad (5)$$

The coherence matrix is obtained in [15]. Polarimetric information of the scattering matrix could be represented by the combination of intensities $|shh|$, $2|shv|$, $|svv|$ in a single RGB image.

2-3-H/A/ α DECOMPOSITION

The newest hybrid approach for uneven surfaces and natural scatterers have been investigated in [16]. To interpret the polarimetric matrices, i.e., the scattering matrix [S] and the coherency matrix [T], there are three polarimetric signatures, which are directly extracted by the eigenvalue analysis of the covariance matrix. The entropy indicates the degree of the statistical disorder of

scattering for high entropy values. A complementary parameter, anisotropy A, is necessary to characterize the set of probabilities. The anisotropy is defined as the relative importance of the second scattering. In fact, using the non-alignment parameter A, the resolution targets exceeds [16, 17].

These parameters are defined as:

$$p_i = \lambda_i / \sum_{i=1}^3 \lambda_i \quad (6)$$

and

$$\alpha = \sum_{i=1}^3 p_i \alpha_i, H = -\sum_{i=1}^3 p_i \log_3(p_i), A = \frac{P_2 - P_3}{P_2 + P_3} \quad (7)$$

where;

$$0 \leq \alpha \leq 90, 0 \leq H \leq 1, 0 \leq A \leq 1 \quad (8)$$

In this equation, P_i is the probability of λ_i . The α -angle varies between zero and 90 degrees corresponding to the type of scatterers.

Due to this definition, the depolarization of the scattered wave is shown through irregularity H, and is expressed by the eigenvalues restricted to $0 \leq H \leq 1$. The entropy can be interpreted as a measure of the randomness of the scattering process. For example, the entropy H increases when surface roughness increases. $H=0$ indicates that the coherency matrix has only one nonzero eigenvalue ($\lambda_1 \neq 0, \lambda_2 = \lambda_3 = 0$) and represents one deterministic scattering process. $H=1$ means that all eigenvalues are equal and represent a random scattering process.

The combination of these parameters provides a useful physical representation namely the classification plane H-A- α . By using this plane, the eight usable classes, denoting an individual type of the scattering mechanism independently of particular data set, can be suggested [16, 17]. Wherever these parameters possess random variables in the scattering of natural targets, a statistical assessment is essentially required.

There are several statistical models to estimate the polarimetric matrices in inverse problems. Among these models, the Wishart Distribution (WD) is a robust technique, which is useful for multi-dimensional synthetic aperture radars (MD-SAR) [10]. In M-dimensional SAR, the target vectors possess m independent elements, and therefore, their polarimetric matrices have M^2 elements. Whereas these elements may not be correlated, a general form of WD must be used.

2-4-EXPERIMENTS BY USING THE NASA/JPL AIRSAR IMAGE

SAR AIR BORN FEATURES

A radar image represents the radar backscatter for the area on the ground; bright features mean that a large fraction of energy was reflected back to the radar, while dark features imply that very little energy was reflected.

Backscatter will also differ depending on different polarizations. AIR SAR transmits pulses in horizontal (H) and vertical (V) polarizations and receives in both H and V, with the resultant combinations of HH, VV, HV or VH. Such polarimetric SAR (Pol. SAR) data have been used to retrieve a variety of useful information such as land cover, land use, and soil moisture. Also, the data gathered by AIRSAR sensors, were developed by NASA-JPL to acquire repeat track SAR data. It provides differential interferometry measurements to estimate surface deformations. The key parameters of the airborne sensor's AIRSAR instruments are given in Table 1 [19]. The data relay boards also represent critical parts of the system. On the flight side one accesses the stored AirSAR data via a fiber channel interface and on the ground it returns the serial data stream for processing or further storage. It provides the ability to overlay the physical link layer with protocol to ensure a quality of service to the data. The data set are extracted by AIRSAR format and San Francisco Bay (CA, US), STK-MLC format with no header: 900rows \times 1024columns and processed in the POLSARPRO.

TABLE 1. SENSOR SPECIFICATIONS

Parameter	dB
TX Power	26 dBm
TX losses	-2.5 dB
RX Gain	2.2dB
Receiver losses	125.7 dB
Background	-0.7 dBm
Required signal	-30 dBm
Link Margin	29 dB

3-RESULTS

3-1- SAR DATA PROCESSING

It can be seen that entropy arises as a natural measure of the inherent reversibility of the scattering data; anisotropy can describe how the data of the reflected wave change with the direction, and that, α can be used to identify the underlying average scattering mechanism. Figure 1 presents an example in San Francisco area.

In this case, the scattering mechanism polarimetric parameters A, H/ α disorder is simulated, and finally, the results of this classification distribution are compared with data. The distribution of the different objectives, based on the combination of each of these parameters in the study area, obtained distribution functions in the interval, and also. Indeed, in this paper, a combination of the two parameters A- α are used, and then, the two

parameters A–H are combined to classify the objectives of the San Francisco Bay area.

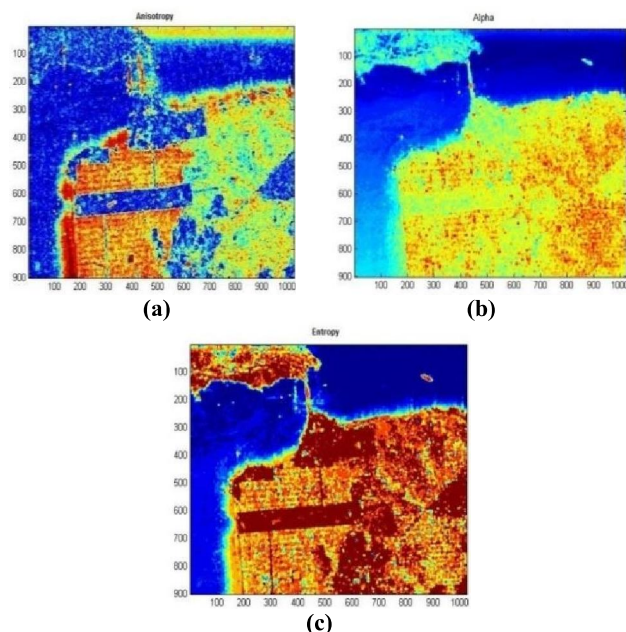


Fig. 1. Polarimetric decomposition main parameters: (a) scattering mechanism α , (b) anisotropy A and (c) entropy H.

3-2- TARGET CLASSIFICATION

A– α BASED SEGMENTATION

A– α classification plane is sub-divided into 6 basic zones based on the characteristic of different scattering behaviors. The basic scattering mechanism of each pixel of the polarimetric SAR image can be identified by comparing its anisotropy using fixed thresholds. The different class boundaries, in the A– α plane, have been determined in form of Single bounce scattering surface reflection (SR), volume diffusion (VD) and double bounce reflection (DB) along the α axis and low, medium and high degree of randomness along the anisotropy axis.

Data distribution in the A– α plane is shown in Figure 2, for the considered scene, and distinct natural clusters, according to a single scattering mechanism class. Therefore, identification results may highly depend on segmentation thresholds. It can be seen, that the largest densities in the occurrence plane correspond to volume diffusion and double bounce scattering with moderate and high randomness. Medium and low entropy surface scattering mechanisms are also frequently encountered in the scene under examination.

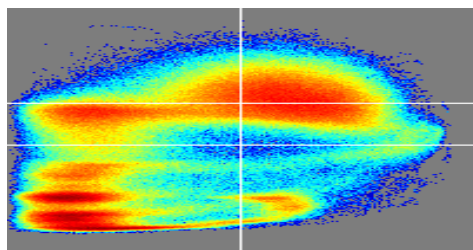


Fig. 2. A_ α segmented plane

A– α LOOK-UP TABLE

In this section, a new look-up table is presented for the above classification method for the first time. This table is obtained by considering Wishart Distribution and the processed image due to Pauli method, and comparing theoptical image and the radar image of San Francisco Bay area. This new look-up table is depicted in Table 2 indeed, each segment represents a special region with its own values of A and α . A more accurate target classification is presented in Table 2 for any values of A between 0 and 1, and α from 0 to 90. This table allows us to define the types of scatterers for any other radar images. Therefore, this method, which has never been proposed before, can be used to classify any unknown targets in radar images. The results in Table 2 shows Subscribed range images obtained from A and Alpha. Consequently, Table 2 states that for $0 < \alpha < 48$, the targets are of the type of single bounce scattering, and by increasing α , the targets approach volume scattering and double bounce scattering types.

TABLE 2. SCATTERER TYPES

α	anisotropy	scatterer type	sample region
$0 < \alpha < 28$	$0 < A < 0.32$	Single bounce scattering	Deep water
$0 < \alpha < 28$	$0.32 < A < 0.56$	Single bounce scattering	Shallow water
$0 < \alpha < 28$	$0.56 < A < 0.79$	Single bounce scattering	Offing region
$28 < \alpha < 45$	$0 < A < 0.5$	Single bounce scattering	Mountainous
$28 < \alpha < 48$	$0.56 < A < 0.75$	Single bounce scattering	Pavement surface
$15 < \alpha < 38$	$0.75 < A < 1$	Single bounce scattering	Coast region
$44 < \alpha < 55$	$0.1 < A < 0.45$	Volume scattering	Forest
$54 < \alpha < 68$	$0.55 < A < 0.9$	Double bounce scattering	Building region
$60 < \alpha < 78$	$0.32 < A < 0.54$	Double bounce scattering	Vegetation
$60 < \alpha < 82$	$0.58 < A < 0.88$	Double bounce scattering	Spares vegetation
$68 < \alpha < 90$	$0.1 < A < 0.34$	Double bounce scattering	No effect region

A – H BASED SEGMENTATION

The other method to classify the targets is obtained by using a combination of the wo parameters A–H. Figure 3 presents A–H color code, segmented plane, and occurrence for the San Francisco Bay area. In this regard, the Pauli decomposition and Wishart decomposition methods are used. Figure 3 shows that the targets are in five regions due to the values of A and H. By using this technique and the classification mentioned in the previous section, unknown targets can be detected in radar images.

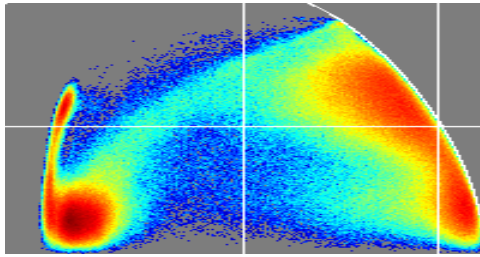


Fig. 3. H_A segmented plane

A-H LOOK-UP TABLE

This section represents the look-up table released by utilizing this method, in which Deterministic scatterers and partial scatterers are shown for different values of A, H, and the types of targets. To do the classification thoroughly, for the whole plane of radar image, the look-up table plane has been divided into 80 sections due to the values of A and H. Each section contains definite A and H values. Actually, the look-up table plane includes all the details of the region. In addition, Table 3 shows that for $0 < H < 0.48$, the scatterers are of the type of deterministic scatterers and by increasing H, the targets approach Partial Scatterers type, and consequently, the targets are classified via the proposed method.

TABLE 3. SCATTERER TYPE AND SAMPLE BY DIFFERENT VALUES OF A, H

entropy	anisotropy	scatterer type	sample region
$0 < H < 0.23$	$0 < A < 0.3$	Deterministic Scatterers	Deep water
$0 < H < 0.23$	$0.3 < A < 0.6$	Deterministic scatterers	Shallow water
$0 < H < 0.23$	$0.6 < A < 0.94$	Deterministic scatterers	Offing region
$0.23 < H < 0.4$	$0.12 < A < 0.35$	Deterministic scatterers	Dipole structure
$0.23 < H < 0.48$	$0.56 < A < 0.82$	Deterministic scatterers	Coast region
$0.43 < H < 0.56$	$0.12 < A < 0.32$	partial scatterers	Mountainous
$0.55 < H < 0.67$	$0 < A < 0.55$	partial scatterers	Roughness region
$0.5 < H < 0.7$	$0.55 < A < 0.85$	partial scatterers	Building /city region
$0.83 < H < 1$	$0 < A < 0.35$	partial scatterers	Dihedral scatterer
$0.75 < H < 1$	$0.56 < A < 0.78$	partial scatterers	Branch / crown structure
$0.67 < H < 0.8$	$0.15 < A < 0.48$	partial scatterers	Forestry / Vegetation
$0.6 < H < 1$	$0.75 < A < 1$	partial scatterers	No effect region

COMPARISON

For best showing of innovation in this paper the simulation results for the Foulum Denmark and Random showcase the San Francisco Bay Area were also compared. Figure 4 shows the Pauli method implemented image of Foulum area. In figure 5 and figure 6, comparison between Foulum Denmark and San Francisco bay area, at the combination of A-Alpha and A-H have been shown. As can be seen Foulum areas show a different structure rather than San Francisco Bay.

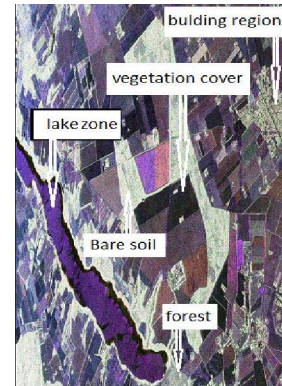
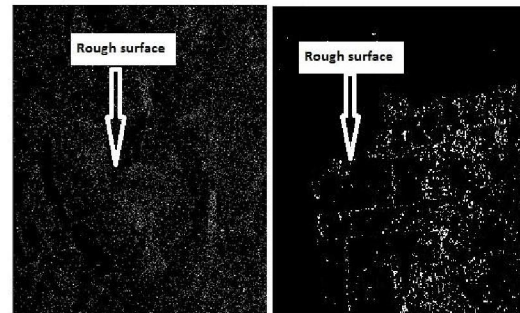
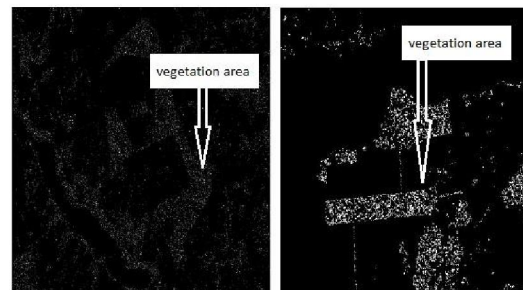


Fig. 4. Pauli method implemented image of Foulum area



A=0.75, $\alpha=40$



A=0.35, $\alpha=62$

Fig. 5. Foulum (left), San Francisco (right)

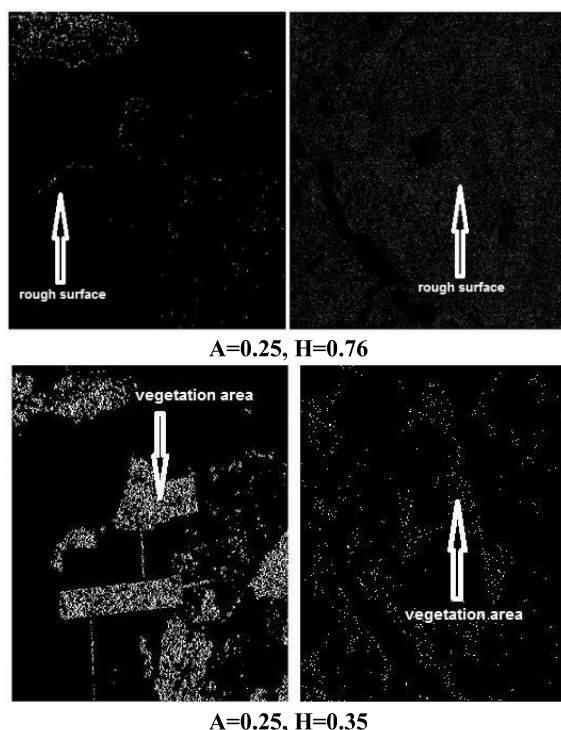


Fig .6. Foulum (left), San Francisco (right)

4-CONCLUSION

In this paper, we have studied the polarimetric signatures such as the α -angle, entropy H and anisotropy A. For this end, a new method has been proposed to classify SAR images due to the combination of the scattering mechanism parameters of A/α and H/A . These parameters have been obtained by collecting the raw data from European Space Agency (ESA). The results are presented by using target decomposition and considering Pauli decomposition and Wishart distribution. More over as an example, the radar image of San Francisco Bay area, which was classified by H- α method before, is classified by applying H-A, A- α methods and for evaluate the efficiency of this new simulation method, simulated San Francisco Bay area is compared to New area Foulum Denmark and the results indicate acceptable accuracy in identifying common goals in the simulated regions. These novel methods led us to new look-up tables, which can be used to classify SAR images when the parameters are known. Actually, the SAR image is not needed to classify in comparison to other methods. Finally it is possible to conclude that the technique proposed in this study is an efficient method for target recognition in SAR applications.

REFERENCES

[1] Storvold, R., E. Malnes, and Y. Larsen, "SAR remote sensing of snow parameters in Norwegian areas-current status and future perspective," *Journal of Electromagnetic Waves and Applications*, Vol. 20, No. 13, 1751–1759, 2006.

[2] Chan, Y. K. and S. Y. Lim, "An introduction to Synthetic Aperture Radar (SAR)," *Progress in Electromagnetics Research*, Vol. 2, 27–60, 2008.

[3] Storvold, R., E. Malnes, Y. Larsen, K. A. Hogda, and S. E. Hamran, "SAR remote sensing of snow parameters in Norwegian areas-current status and future perspective," *Journal of Electromagnetic Waves and Applications*, Vol. 20, No. 13, 1751–1759, 2006.

[4] Nie, X., D. Y. Zhu, and Z. D. Zhu, "Application of synthetic bandwidth approach in SAR polar format algorithm using the decamp technique," *Progress in Electromagnetics Research*, PIER 80, 447–460, 2008.

[5] Wu, B.-I., M. Yeung, and Y. Hara, "In-SAR high in version by using 3-D phase projection with multiple baselines," *Progress In Electromagnetics Research*, PIER 91, 173–193, 2009.

[6] Lim, T. S., C.-S. Lim, and V. C. Koo, "Autofocus algorithm performance evaluations using an integrated SAR product simulator and processor," *Progress In Electromagnetics Research*, PIERB, Vol. 3, 315–329, 2008.

[7] Ebrahimi-Ganjeh, M. A. and A. R. Attari, "Study of water bolus effect on SAR penetration depth and effective field size for local hyperthermia," *Progress In Electromagnetics Research*, PIER, B, Vol. 4, 273–283, 2008.

[8] S. R. Cloude, E. Pottier. "An entropy based classification scheme for land applications of Polarimetric SAR. *IEEE Transactions on Geoscience and Remote Sensing*, vol. 35, 1997, PP.549-557.

[9] J .S Lee, Mo. & Grunes. Unsupervised classification using Polarimetric decomposition and the complex Wishart classifier. *IEEE Transactions on Geoscience and Remote Sensing* vol.137,1999,PP.2249-2258.

[10] E. Pottier. Unsupervised classification scheme and topography derivation of POLSAR data based on the $H/\alpha/A$ polarimetric decomposition theorem. In *Proc. 4th International workshop on Radar Polarimetry* .PP.535-548, Nantes, France, July 1998.

[11] Cloude, S. R., J. Fortuny, J. M. Lopez-Sanchez, and A. J. Sieber, "Wide-band polarimetric radar inversion studies for vegetation layers," *IEEE Transactions on Geoscience and Remote Sensing*, Vol. 37, No. 5, 2430–2441, 1999.

[12] Lopez-Martinez, C., E. Pottier, and S. R. Cloude, "Statistical assessment of eigenvector-based target decomposition theorems in radar polarimetry," *IEEE Transactions on Geoscience and Remote Sensing*, Vol. 43, No. 9, 2058–2074,

2005.

- [13] Cloude, S. R. and E. Pottier, "A review of target decomposition theorems in radar polarimetry," IEEE Transactions on Geoscience and Remote Sensing, Vol. 34, No. 2, 498–518, 1996.
- [14] J. S. Lee, M. R. Grunes. Unsupervised terrain classification preserving Polarimetric scattering characteristics. IEEE Transactions on Geoscience and Remote Sensing, vol.42, 2004, PP.722-731.
- [15] Zhao Li-wen, Zhou Xiao-guang, Jiang Yong-mei, Kuanggangyao. "Iterative Classification of Polarimetric SAR Image Based on the Freeman Decomposition and Scattering Entropy". IEEE Transactions On Geoscience And Remote Sensing, vol. 7, 2007, PP.473-476.
- [16] B. Zakeri, A. Ghorbani, and H. Amindavar "A new method to extract the polarimetric parameters in imaging radars," Progress In Electromagnetics Research, PIER 87, pp 167–182, 2008.